Medical Research Archives

European Society of Medicine

OPEN ACCESS

Published: November 30, 2023

Citation: Okada, Y., et al., 2023. Role of Integrins Involved in Mn^{2+}-Dependent Adhesion to Fibronectin Peptide of Mastocytoma P-815 Cells and Peritoneal Mast Cells. Medical Research Archives, [online] 11(11). https://doi.org/10.18103/mra.v11i11.4683

Copyright: © 2023 European Society of Medicine. This is an open-access article distributed under the terms of the Creative Commons Attribution License, which permits unrestricted use, distribution, and reproduction in any medium, provided the original author and source are credited.

DOI: https://doi.org/10.18103/mra.v11i11.4683

ISSN: 2375-1924

RESEARCH ARTICLE

Role of Integrins Involved in Mn^{2+}-Dependent Adhesion to Fibronectin Peptide of Mastocytoma P-815 Cells and Peritoneal Mast Cells

Yasuyo Okada[1]*, Kiyomi Ueyama[1], Jyun-ichi Nishikawa[1], Atsushi Ichikawa[1,2]

[1]School of Pharmacy and Pharmaceutical Sciences, Mukogawa Women's University, 11-68 Koshien Kyuban-cho, Nishinomiya, Hyogo 663-8179, Japan. [2]Bio-Education Laboratory, Tawara Building #702, 1-21-33 Higashinakajima, Osaka 533-0033, Japan.

*okada@mukogawa-u.ac.jp

ABSTRACT

Mn^{2+}-dependent integrin-mediated adhesion to the extracellular matrix is extensively studied, however, its implication in mast cell biology remains unexplored. This study aims to investigate the role of Mn^{2+} in promoting adhesion in mouse mastocytoma P-815 cells (P-815) and peritoneal mast cells (PMC) to the Arg-Gly-Asp (RGD)-enriched fibronectin peptide (RGD matrix) within the culture medium. Our findings indicate that Mn^{2+} induces cell adhesion, with optimal results achieved when P-815 were exposed to 2 mM Mn^{2+} for 30 min at 37°C, resulting in approximately 40% cell adhesion to the RGD matrix. The Mn^{2+}-dependent P-815 adhesion was inhibited by anti-integrin α4, β1, and β3 subunit function-blocking antibodies, and by the integrin αIIbβ3 antagonist tirofiban, indicating the involvement of integrins α4β1 and αIIbβ3. Similarly, Mn^{2+}-dependent PMC adhesion to the RGD matrix was inhibited by anti-integrin α4, α5, β1, β3, and β7 subunit function-blocking antibodies and tirofiban, demonstrating the involvement of integrins α4β1, α4β7, α5β1, and αIIbβ3. Integrins α4β1 and αIIbβ3 were consistently involved in Mn^{2+}-induced adhesion reactions in both P-815 and PMC, while integrins α4β7 and α5β1 were specifically implicated in the response to PMC only. The addition of the actin inhibitor cytochalasin D, glycosylphosphatidylinositol-anchored protein (GPI-AP) cleaving enzyme phosphatidylinositol-specific phospholipase C, and the PKA inhibitor H-89 significantly reduced Mn^{2+}-dependent P-815 adhesion to the RGD matrix. However, adding the myosin II inhibitor brebbistatin and the RhoA inhibitor Y27632 did not produce the same effect. Furthermore, cellular cholesterol removal with 6-*O*-α-maltosyl-β cyclodextrin significantly diminished Mn^{2+}-dependent P-815 adhesion, concomitant with a decrease in the expression of integrin α4 and β1 subunits on the cell surface.

In summary, Mn^{2+} fosters adhesion to the RGD matrix through integrins α4β1 and αIIbβ3, which are common between P-815 and PMC, while integrins α4β7 and α5β1 are specifically involved in PMC adhesion. The Mn^{2+}-induced adhesion reaction in P-815 closely correlates with signal expression, including cAMP/PKA, GPI-AP, cellular cholesterol, and actin cytoskeleton, demonstrating a correlation between Mn^{2+}-induced P-815 adhesion and signaling pathways within lipid rafts. These results may clarify questions regarding adhesion and detachment of mast cells to the extracellular matrix involved in metal ion-induced immunity and inflammation suppression.

Keywords: manganese, integrin, cell adhesion, mastocytoma P-815 cells, mast cells, lipid rafts.

1. Introduction

Integrins are a family of α/β heterodimeric adhesion metalloprotein receptors with 18α and 8β subunits that can assemble into 24 distinct receptors with different binding properties and tissue distributions[1,2]. The α- and β-subunits are constructed from several domains with flexible linkers. Integrin receptors usually adopt an inactive conformation with low affinity for their extracellular ligands, which are converted into the active form by intracellular and extracellular signals[3]. The affinity of integrins for ligands is controlled through a process termed integrin activation and the *de novo* synthesis[4]. Integrin activation is regulated by conformational changes caused by binding of divalent metal ions such as Mg^{2+}, Ca^{2+}, and Mn^{2+};[3,5] via structural changes of lipid rafts in the membranes; and modification of extracellular matrix (ECM) components such as actin fibers[6]. Among these processes, the binding interactions of divalent metal ions have been studied extensively at the molecular level of integrins[3,5]. The divalent metal ions bind to the metal ion-dependent adhesion site (MIDAS) of the αI domain in the integrin α subunit and the βI domain in αI domain-less integrins[3,5]. While Mg^{2+} occupies the central site, Ca^{2+} occupies the flanking sites of MIDAS[7,8]. Mg^{2+} is assigned to the central site, and Ca^{2+} is assigned to the flanking sites of MIDAS[7,8]. Importantly, Ca^{2+} binding to these adjacent sites has an inhibitory effect[9,10]. In contrast, the binding of Mn^{2+} induces conformational changes in ligand binding sites, resulting in the activation of integrin[11-13]. However, despite our knowledge of Mn^{2+} activation, the specific signaling events triggering Mn^{2+}-dependent cell adhesion remain unclear. Integrin signaling is intricately linked to the composition and organization of lipid rafts within the plasma membrane. These lipid rafts serve as critical regulators of cellular function, influenced by activated integrins through interactions with signaling molecules and the ECM[6]. Lipid rafts are complex microdomains rich in cholesterol, sphingolipids, and various proteins, including glycosylphosphatidylinositol-anchored proteins (GPI-AP) and signaling components involved in cell adhesion to the ECM, as well as ECM-mediated cell migration[14]. Surprisingly, little research has delved into understanding how Mn^{2+} affects cell adhesion concerning the interplay of key signaling components, including integrins and lipid rafts.

Mast cells are inflammatory and immunoregulatory cells that reside in tissues. Based on the difference in proteoglycans contained in the granules, mast cells in animals can be differentiated into two types: mucosal mast cells (MMC) and connective tissue mast cells (CTMC). According to this classification, mouse mastocytoma P-815 cells (P-815) belong to the MMC category, and mouse peritoneal mast cells (PMC) belong to the CTMC category. The growth and differentiation of progenitor mast cells are controlled by multiple factors[15,16]. Soluble factors like stem cell factors and various cytokines have been identified alongside insoluble factors, including components of the ECM such as collagen, fibronectin, hyaluronic acid, and laminin. Our prior research has shown that P-815 when cultivated in suspension, acquire adhesive properties upon exposure to prostaglandin E_2 (PGE_2) within the Arg-Gly-Asp (RGD)-enriched

peptide of fibronectin (RGD matrix)[4,17]. Notably, PGE_2-induced adhesion in P-815 is associated with the *de novo* synthesis of the integrin β3 subunit, resulting in increased surface expression levels of integrins αIIbβ3 and αvβ3[4]. However, limited studies have suggested a role for Mn^{2+} in mast cell-ECM adhesion. These studies include mast cell migration and tissue organization, which depend on integrin-ECM interaction[18]. Additionally, there is evidence of hypoxia modulating human mast cell adhesion to hyaluronic acid through CD44 in inflammatory and immune processes[19]. Moreover, Mn^{2+} has been found to promoting adhesion of S39T-bone marrow-derived mast cells (BMMC) expressing integrin αEβ7 and E-cadherin to the monolayer of E-cadherin+F9 cells[20]. Despite these findings, the existing knowledge cannot fully account for promoting adhesion via integrin in mast cells by Mn^{2+}.

Therefore, this study aimed to clarify the specific molecular species of integrins involved in Mn^{2+}-induced adhesion to the RGD matrix of P-815 and PMC. Furthermore, this research elucidates the signaling pathways by Mn^{2+} in integrin-mediated P-815 adhesion.

2. Materials and Methods

2.1. Animals:

Specific pathogen-free, 9-week-old male ddY mice were obtained from Japan SLC (Hamamatsu, Japan). All animal experiments were performed in accordance with the Animal Experiments Guidelines of Mukogawa Women's University and approved by the Animal Experiment Committee.

2.2. Materials:

ProNectin-F™, a protein polymer containing multiple copies of the RGD sequence from human fibronectin and an RGD-enriched matrix fragment, was procured from Sanyo Chemical Industries (Kyoto, Japan). Fisher's medium was sourced from ICN Biomedicals (Irvine, CA, USA), while fetal calf serum (FCS) was obtained from Biowest (Nuaillé, France). Cycloheximide was purchased from Merck Calbiochem (Darmstadt, Germany), and the fibronectin active fragment (GRGDS) was procured from the Peptide Institute (Osaka, Japan). Phosphatidylinositol-specific phospholipase C (PI-PLC) from *Bacillus cereus* [EC 3.1.4.10][21], H-89, Y27632, and blebbistatin were sourced via Sigma (St. Louis, MO, USA), and tirofiban was obtained from Toronto Research Chemicals (Toronto, Canada). Integrin function-blocking monoclonal antibodies (mAbs), including anti-α4 mAb, anti-α5 mAb, anti-αv mAb, anti-β1 mAb, anti-β2 mAb, anti-β3 mAb and anti-β7 mAb, as well as all isotype-matched negative controls, were supplied by Becton Dickinson Biosciences (San Jose, CA, USA). Anti-CD47 mAb was purchased from Thermo Fisher Scientific (Waltham, MA, USA). The production of 6-*O*-α-maltosyl-β cyclodextrin (Mal-βCD) involved maltose and βCD, enzymatically processed using *Pseudomonas* isoamylase (EC 3.2.1.68) and purified to a degree exceeding 99.8% according to a published procedure[22]. All other reagents used met guaranteed or liquid chromatography/mass spectrometry (LC/MS) grade standards.

2.3. Cell Culture and Cell Viability Assay:

P-815 were maintained in suspension culture in Fisher's medium containing 10% heat-inactivated FCS at 37°C in a CO_2-humidified atmosphere[17]. Cell viability was determined using the trypan blue exclusion method.

2.4. Measurement of P-815 Adhesion:

The 24-well tissue culture plates were prepared by coating them with 10 μg/mL ProNectin-F™, following established procedures[17]. To conduct the adhesion assay, 0.5 mL of P-815 (5 × 10^5 cells/mL) were seeded into each well and incubated in an FCS culture medium for 20 hr at 37°C, after which they were subjected to incubation in the presence or absence of test compounds for varying durations. After removing the floating cells through aspiration, the adherent cells were harvested by treating them with phosphate-buffered saline (PBS) containing 0.02% ethylenediaminetetraacetic acid (EDTA) and 0.25% trypsin at 37°C for 5 min. Subsequently, the collected cells were resuspended in PBS containing 0.02% EDTA and 2% FCS. The number of non-adherent and adherent cells was counted using a Coulter Z1 cell counter (Beckman Coulter, Brea, CA, USA). The percentage of adherent cells was calculated using the formula: cell adhesion (%) = number of adherent cells × 100/(number of adherent cells + number of non-adherent cells).

2.5. Purification of PMC:

PMC recovery followed established procedures[23]. The purity of the obtained PMC was confirmed to be at least 95% pure through Alcian blue/Safranin-O staining.

2.6. Measurement of PMC Adhesion:

The adhesion of the PMC was measured following a previously established protocol with slight modifications[23]. A glass-bottom dish (Cellvis, Mountain View, CA, USA) was coated with 10 μg/mL ProNectin-F™. PMC was suspended in Tyrode-4-(2-hydroxyethyl)-1-piperazineethanesulfonic acid (Tyrode-HEPES) buffer containing 0.1% bovine serum albumin (BSA) and then seeded onto the glass-bottom dish at a density of 3 × 10^4 cells per dish. The cells were incubated for 30 min at 37°C before stimulation. The adherent cells were rinsed with Tyrode-HEPES buffer containing 0.1% BSA, fixed with a solution containing 100 mM sodium phosphate (pH 7.4), 3% sucrose, 2% paraformaldehyde, and 0.1% glutaraldehyde, and subsequently stained with acidic toluidine blue.

2.7. Preparation of Inclusion Complex of Cholesterol with Mal-βCD:

The inclusion complex of cholesterol with Mal-βCD (Cho/Mal-βCD) was prepared using the solubility method described previously[24]. Briefly, after incubation with excess amounts of cholesterol and 1 mM Mal-βCD in an FCS-free medium at 37°C for 1 hr, the reaction mixture was filtered through a 0.2 μm membrane filter (Millipore, Billerica, MA, USA) to remove any undissolved cholesterol. The cholesterol concentration in Cho/Mal-βCD was 15 μM as determined by LC/MS.

2.8. Reduction of Cellular Cholesterol with Mal-βCD and Cholesterol Loading with Cho/Mal-βCD:

The reduction of cellular cholesterol by Mal-βCD was performed as follows: P-815 (2 × 10^6 cells/assay) in 0.5 mL of FCS-free medium were incubated with 5 mM Mal-βCD at 37°C for 15 min or 30 min. The cells were collected by centrifugation, washed twice with ice-cold PBS, homogenized in 2-propanol using a Sonifier (BRANSON, Kanagawa, Japan), and subsequently analyzed by LC/MS.

Cholesterol loading with Cho/Mal-βCD (an inclusion complex composed of 15 μM cholesterol and 1mM Mal-βCD) was

performed as follows: P-815 (2 × 10^6 cells/assay) treated with 5 mM Mal-βCD at 37°C for 30 min were incubated in 0.5 mL Cho/Mal-βCD at 37°C for 15 min or 30 min. The cells were collected by centrifugation, washed twice with ice-cold PBS, homogenized in 2-propanol using a Sonifier, and subsequently analyzed by LC/MS.

2.9. LC/MS Analysis:

LC/MS analysis was conducted using a Quattro Premier triple-quadrupole LC/MS instrument (Micromass, Manchester, UK) equipped with an electrospray ionization source and the Alliance HT Waters 2795 separation module (Waters Co., Milford, MA, USA). Data were processed using MassLynx software (Waters Co.) following the method described previously[25].

2.10. Flow Cytometry:

The expression levels of integrin subunits on the P-815 surface were analyzed using flow cytometry, as previously reported[4,25]. Briefly, P-815 (5 × 10^5 cells) were washed twice with PBS containing 2% FCS (2% FCS/PBS) and incubated with rat anti-mouse CD16/CD32 mAb (1:30 in 2% FCS/PBS) in order to block nonspecific binding sites for 1 hr. The cells were washed with 2% FCS/PBS and incubated with the appropriate anti-mouse integrin mAb (FITC- or PE-conjugated, 1:80 in 2% FCS/PBS) for 30 min. The anti-mouse integrin mAbs used were PE-conjugated anti-α2 mAb, FITC-conjugated anti-α4 mAb, PE-conjugated anti-α5 mAb, PE-conjugated anti-αIIb mAb, PE-conjugated anti-αv mAb, FITC-conjugated anti-β1 mAb, PE-conjugated anti-β2 mAb, PE-conjugated anti-β3 mAb, and FITC-conjugated anti-β7 mAb. All mAbs were sourced from Becton Dickinson Biosciences. The cells were washed twice with 2% FCS/PBS, and the cell pellet was resuspended in 2% FCS/PBS. All procedures were performed at 4°C. The samples were then analyzed using a FACScan flow cytometer (Nippon Becton Dickinson, Tokyo, Japan) with CellQuest Pro software (Nippon Becton Dickinson) as previously described.

2.11. Statistical Analysis:

Data are shown as mean ± standard deviation (SD) of three or more experiments. Comparisons between the two groups were made using the Student's *t*-test. A one-way analysis of variance was first performed to compare more than two groups with comparable variances, and Dunnett's test was then used to evaluate pairwise group differences. A value of $^{**}p < 0.01$ was considered significant.

3. Results

3.1. Effects of Divalent Metal Ions on P-815 Adhesion to RGD Matrix:

The effect of various divalent cations, including Mn^{2+}, on P-815 adhesion to the RGD matrix was assessed in Fisher's medium, which contained 0.6 mM Ca^{2+} and 0.5 mM Mg^{2+} (Fig. 1). Among these cations, Mn^{2+} demonstrated the most significant adhesion activity, followed by a modest activity for Co^{2+} and Ni^{2+}, while Ca^{2+} and Mg^{2+} exhibited no notable activity.

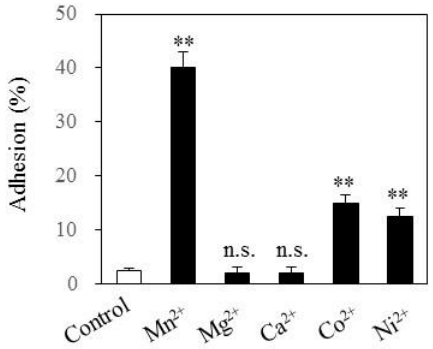

Fig. 1. Effect of different divalent metal ions on P-815 adhesion to RGD matrix. P-815 were incubated in Fisher's culture medium containing 0.6 mM Ca^{2+} and 0.5 mM Mg^{2+} with or without 2 mM each of $MnCl_2 \cdot 4H_2O$, $CaCl_2 \cdot 2H_2O$, $MgCl_2 \cdot 6H_2O$, $CoCl_2 \cdot 6H_2O$, or $NiCl_2 \cdot 6H_2O$ for 30 min at 37°C. The number of adherent P-815 was measured as described in "materials and methods." $^{**}p < 0.01$ vs. control; n.s., not significant.

3.2. Concentration- and Time-Dependence of Mn^{2+}-Induced P-815 Adhesion to RGD Matrix:

The effect of Mn^{2+} on P-815 adhesion exhibited a dose-dependent pattern, reaching a plateau at 2 mM and maintaining that level up to 4 mM (Fig. 2A). Conversely, the Mn^{2+} (2 mM)-induced P-815 adhesion response displayed a linear increase within the first 20 min, followed by a gradual decline after reaching the plateau (Fig. 2B).

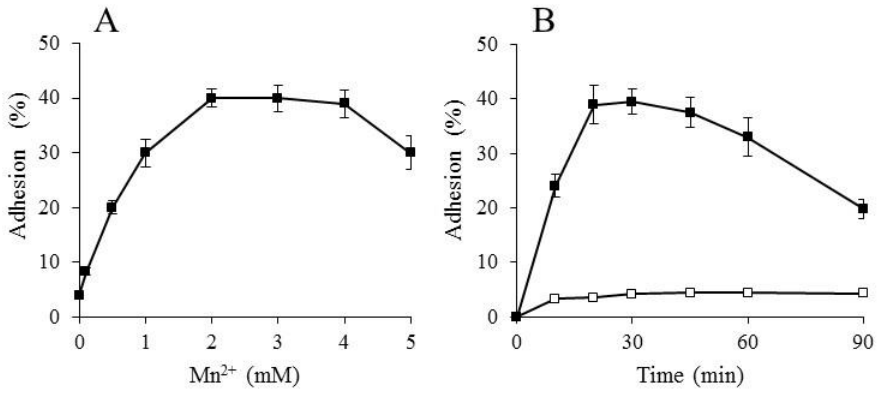

Fig. 2. Concentration and time dependence of Mn^{2+}-induced P-815 adhesion response to RGD matrix. (A) Effect of Mn^{2+} concentration on Mn^{2+}-induced P-815 adhesion. P-815 were incubated with or without $MnCl_2 \cdot 4H_2O$ at the indicated dose for 30 min at 37°C. (B) Effect of reaction time on Mn^{2+}-induced P-815 adhesion. P-815 were incubated with 2 mM $MnCl_2 \cdot 4H_2O$ for the indicated times at 37°C. In (A) and (B), the number of adherent P-815 was measured as described in "materials and methods."

3.3. Effects of EDTA, Ca^{2+}, or GRGDS Addition on Mn^{2+}-Induced P-815 Adhesion to RGD Matrix:

As depicted in Fig. 3A, EDTA exhibited a dose-dependent inhibition of Mn^{2+}-induced P-815 adhesion within the concentration range of 0.1 to 1 mM. This suggests that the decrease in Mn^{2+} concentration may be attributed to EDTA, supported by the stability constants of metal-EDTA complexes (log *K* at 20°C: Mn^{2+}: 13.8 > Ca^{2+}: 10.7 > Mg^{2+}: 8.7)[26]. Furthermore, high concentrations of Ca^{2+} were observed to have suppressive effects, as the addition of 2 mM Ca^{2+} to the medium

containing 0.6 mM Ca^{2+} resulted in a final concentration of 2.6 mM Ca^{2+}, leading to the inhibition of Mn^{2+}-induced P-815 adhesion (Fig. 3B). The ligand in the experimental system was verified to be an RGD peptide derived from fibronectin, as demonstrated by the addition of GRGDS, a competitive antagonist of the RGD sequence.

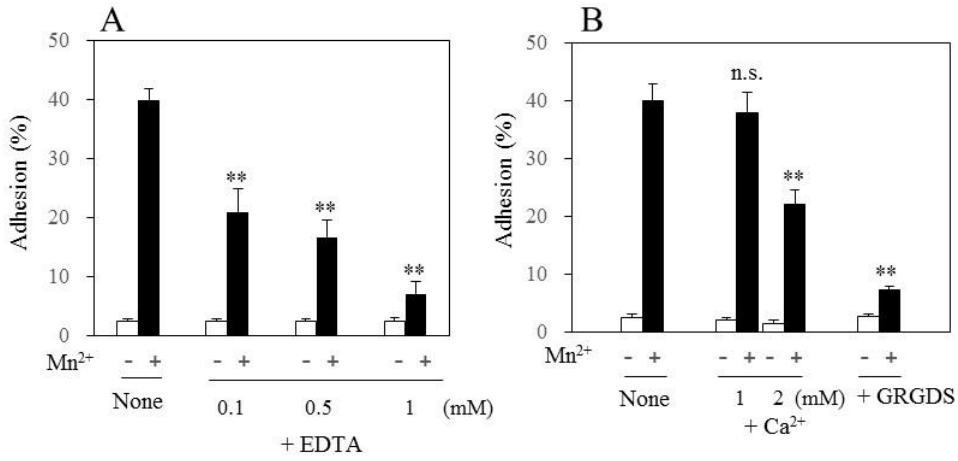

Fig. 3. Effects of EDTA, Ca^{2+}, or GRGDS addition on Mn^{2+}-induced P-815 adhesion to RGD matrix. (A) Effect of EDTA on Mn^{2+}-induced P-815 adhesion. P-815 were incubated with or without 0.1, 0.5, or 1 mM EDTA for 30 min at 37°C, followed by 2 mM $MnCl_2 \cdot 4H_2O$ for 30 min at 37°C. (B) Effects of Ca^{2+} or GRGDS on Mn^{2+}-induced P-815 adhesion. P-815 were incubated with or without 1 or 2 mM $CaCl_2 \cdot 2H_2O$ or 300 μM GRGDS for 30 min at 37°C, followed by 2 mM $MnCl_2 \cdot 4H_2O$ for 30 min at 37°C. In (A) and (B), the number of adherent P-815 was measured as described in "materials and methods." $^{**}p < 0.01$ vs. Mn^{2+}-stimulated cells without EDTA, Ca^{2+}, or GRGDS; n.s., not significant.

3.4. Involvement of Components Associated with Lipid Rafts and Integrins on Mn^{2+}-Induced P-815 Adhesion to RGD Matrix:

To investigate the involvement of lipid raft-associated components in Mn^{2+}-dependent P-815 adhesion, we assessed the % inhibition of the adhesion reaction by introducing inhibitors that target the components or generators associated with these events (Table 1). Our findings suggest that Mn^{2+}-induced P-815 adhesion likely relies on actin polymerization and elongation, as demonstrated by the inhibitory effects of cytochalasin D[27], a known agent for actin depolymerization. Additionally, inhibition by H-89 suggests a requirement for reactions associated with cAMP-dependent protein kinase A (PKA) activity, a known resident of lipid rafts[28], and a mediator of the P-815 adhesion response induced by PGE_2-EP4 addition[17]. Moreover, inhibition by PI-PLC implies the involvement of glycosylphosphatidylinositol-anchored proteins (GPI-AP), known signaling regulators of adhesion molecules in lipid rafts[29]. Cellular cholesterol levels play a crucial role in Mn^{2+}-induced P-815 adhesion, as demonstrated by the significant impact of reduced cellular cholesterol induced by Mal-βCD addition[24] on the adhesion response. However, Mn^{2+}-induced adhesion reactions seem to be unrelated to Rho-associated coiled-coil forming kinase (ROCK) activation and the subsequent myosin phosphorylation, as evidenced by the lack of effect from Y27632, a specific ROCK inhibitor, and blebbistatin, a specific inhibitor of myosin II. Incubation of Mn^{2+}-induced P-815 at 4°C or with sodium

azide or cycloheximide did not affect their adherent ability, indicating that energy metabolism and the *de novo* protein synthesis are unnecessary for Mn^{2+}-dependent events. Additionally, the integrin-associated protein CD47, known to impact cell adhesion, spreading, and migration[30,31], did not appear to correlate with the Mn^{2+}-induced P-815 adhesion response, as suggested by the absence of an anti-CD47 antibody effect.

Table 1 Effects of temperature or various compounds involved in cell metabolism on Mn^{2+}-induced P-815 adhesion to RGD matrix.

Inhibitor or temperature	Inhibitiory effect (%)
Cytochalasin D (1 μg/mL)	87.5 ± 5.2
Mal-βCD (5 mM)	67.6 ± 5.5
PI-PLC (2 U/mL)	60.6 ± 4.8
H-89 (10 μM)	37.5 ± 5.5
Y27632 (10 μg/mL)	5.2 ± 3.8
Blebbistatin (10 μg/mL)	3.3 ± 2.5
Anti-CD47 mAb (30 μg/mL)	4.3 ± 3.5
4°C for 1 hr	8.8 ± 4.5
Sodium azide (2 mM)	10.2 ± 3.8
Cycloheximide (0.1 μg/mL)	15.2 ± 4.8

P-815 were exposed to various inhibitors at the specified concentrations for 30 min at 37°C or 4°C. Subsequently, they were subjected to 2 mM $MnCl_2 \cdot 4H_2O$ treatment for 30 min at the same temperature. The number of adherent P-815 was measured as described in "materials and methods." The adhesion rate in the absence of an inhibitor was considered 100%, and the outcomes with inhibitors are expressed as "Inhibitory effect (%)."

3.5. Identification of Integrin Molecules Involved in Mn^{2+}-Induced Adhesion of P-815 and PMC to RGD Matrix:

In previous studies, we confirmed the steady-state expression of at least eight integrin subunits, namely α4, α5, αIIb, αv, β1, β2, β3, and β7, on the surface of P-815[4,25]. In this investigation, we aimed to identify which specific integrin subunits are essential for P-815 adhesion in response to Mn^{2+} addition. The Mn^{2+}-induced P-815 adhesion reaction was notably hindered by the inclusion of anti-integrin α4, β1, and β3 subunit mAbs, along with the integrin αIIbβ3 antagonist tirofiban, thus implicating the integral involvement of integrins α4β1 and αIIbβ3 (Fig. 4A). In contrast, the Mn^{2+}-induced adhesion reaction of PMC was significantly impaired upon the addition of anti-integrin α4, α5, β1, β3, and β7 subunit mAbs, as well as tirofiban. This suggests the pivotal roles played by integrins α4β1, α4β7, α5β1, and αIIbβ3 in this context (Fig. 4B).

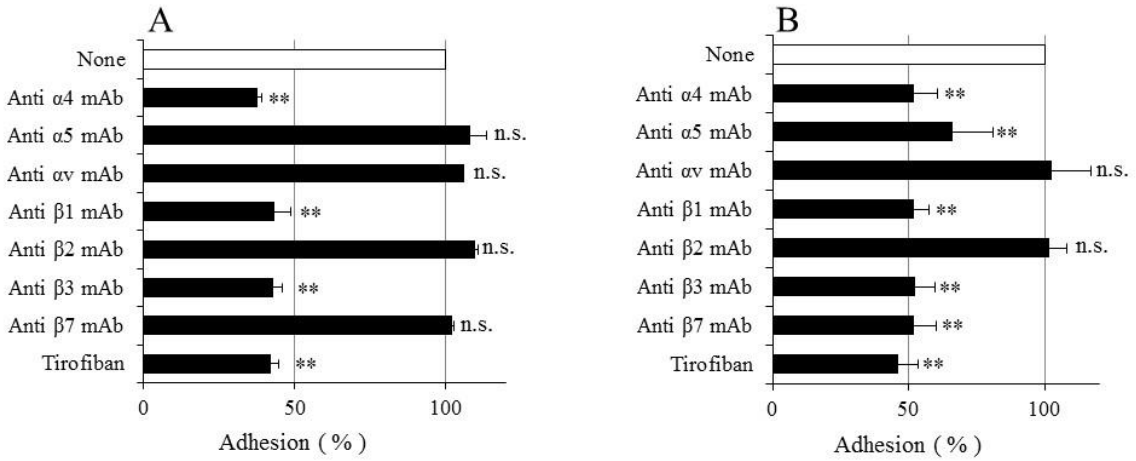

Fig. 4. Effects of anti-integrin mAbs or integrin antagonist on Mn^{2+}-induced P-815 and PMC adhesion to RGD matrix.(A) P-815 were incubated with or without 20 μg/mL of each specific function-blocking anti-integrin mAbs or 50 μM tirofiban for 30 min at 37°C, followed by 2 mM $MnCl_2 \cdot 4H_2O$ for 30 min at 37°C. (B) PMC were seeded on the glass-bottom dish and incubated for 30 min at 37°C. The cells were incubated with or without 20 μg/mL of each specific function-blocking anti-integrin mAbs or 50 μM tirofiban for 30 min at 37°C, followed by 2 mM $MnCl_2 \cdot 4H_2O$ for 30 min at 37°C. In (A) and (B), the number of adherent P-815 or PMC were measured as described in "materials and methods." Adhesion (%) without anti-integrin mAbs or tirofiban with Mn^{2+} represents 100% adhesion. $^{**}p < 0.01$ vs. none; n.s., not significant.

3.6. Effect of Mn^{2+} Addition on P-815 Adhesion Induced by PGE_2 Pretreatment:

In a previous study, we demonstrated that adding PGE_2 promotes P-815 adhesion to the RGD matrix by increasing the *de novo* synthesis of the integrin β3 subunit[4]. This context provides an excellent model for investigating the impact of Mn^{2+} addition on the *de novo* synthesized integrins. Our observations revealed that the PGE_2-induced adhesion response in P-815 initiates at 6 hr and reaches a plateau at 18 hr. Based on this time frame, Mn^{2+} was administered 30 min after the addition of PGE_2 to P-815, specifically at 17.5 hr (Fig. 5). Interestingly, the ratio of P-815 adhesion resulting from the co-addition of Mn^{2+} and PGE_2 was 1.3 times higher than the combined effect of each compound added individually. This outcome suggests that Mn^{2+} influences the *de novo* synthesized integrin β3 subunit, which is stimulated by PGE_2, thereby enhancing cell adhesion capability.

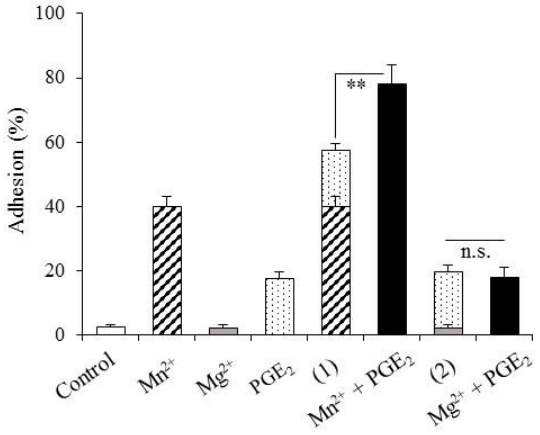

Fig. 5. Effect of PGE_2 on Mn^{2+}-induced P-815 adhesion to RGD matrix. P-815 were incubated with or without 1 μM PGE_2 for 17.5 h at 37°C, followed by incubation with or without 2 mM $MnCl_2 \cdot 4H_2O$ or $MgCl_2 \cdot 6H_2O$ for 30 min at 37°C. The number of adherent P-815 was measured as described in "materials and methods." (1) indicates the sum of the adhesion rates induced by Mn^{2+} alone and PGE_2 alone, and (2) indicates the sum of the adhesion rates induced by Mg^{2+} alone and PGE_2 alone. $^{**}p < 0.01$; n.s., not significant.

3.7. Effects of Mal-βCD and Cho/Mal-βCD on Mn^{2+}-Stimulated P-815 Adhesion to RGD Matrix, and Cell Surface Expression of Integrin α4 and β1 Subunits in P-815:

As mentioned in Section 3.4, Mn^{2+}-dependent P-815 adhesion was found to diminish with a decrease in cellular cholesterol levels resulting from the addition of Mal-βCD. Here, we elucidated the critical relationship between cellular cholesterol levels and cell adhesion in P-815 treated with Mal-βCD and Cho/Mal-βCD. Treatment of P-815 with 5 mM Mal-βCD for 30 min resulted in a 60% reduction in cellular cholesterol levels in a non-cytotoxic manner (Fig. 6). Under these conditions, the addition of Mn^{2+} resulted in a notable decrease in the ratio of Mn^{2+}-induced P-815 adhesion by approximately 68% compared to the control without Mal-βCD (Fig. 7A). Remarkably, these diminished responses were restored when cholesterol was reintroduced upon the addition of Chol/Mal-βCD (Fig. 7A). In parallel with the alterations in cellular cholesterol levels and cell adhesion, the expression levels of integrin α4 and β1 subunits declined upon Mal-βCD treatment and subsequently returned to their original values following the addition of Chol/Mal-βCD (Fig. 7B).

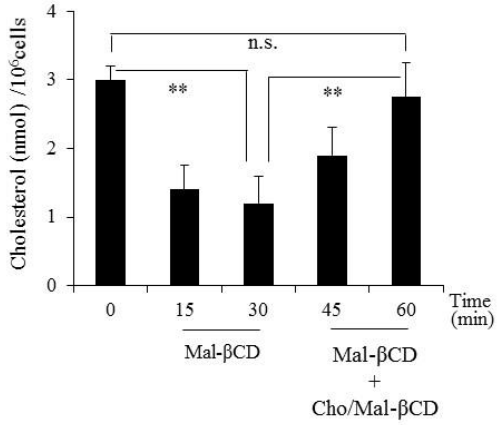

Fig. 6. Effects of Mal-βCD and Cho/Mal-βCD on cellular cholesterol levels of P-815. P-815 were incubated with or without 5 mM Mal-βCD in FCS-free medium for 15 min or 30 min at 37°C, followed by incubation with Cho/Mal-βCD for 15 min or 30 min at 37°C. Cholesterol levels were measured using LC/MS according to the procedure described in "materials and methods." $^{**}p < 0.01$; n.s., not significant.

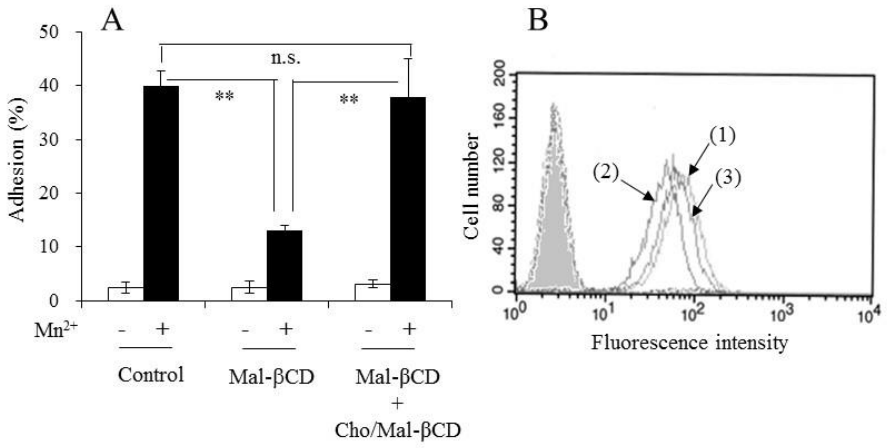

Fig. 7. Effects of cholesterol levels on Mn^{2+}-induced P-815 adhesion to RGD matrix and cell surface expression of integrin β1 subunit in P-815. (A) Effects of Mal-βCD and Cho/Mal-βCD on Mn^{2+}-induced P-815 adhesion. P-815 were pretreated with or without 5 mM Mal-βCD for 30 min at 37°C, followed by exposure to 2 mM $MnCl_2 \cdot 4H_2O$ for 30 min at 37°C, and then followed by cholesterol supplement with Cho/Mal-βCD for 30 min at 37 °C. The number of adherent P-815 was measured as described in "materials and methods." $^{**}p < 0.01$; n.s., not significant. (B) Effects of Mal-βCD and Cho/Mal-βCD on the cell surface expression of integrin β1 subunit in P-815. P-815 were treated with or without 5 mM Mal-βCD in FCS-free medium for 30 min at 37 °C, followed by cholesterol supplement with or without Cho/Mal-βCD for 30 min at 37°C. The cell surface expression level of integrin β1 subunit was determined by FACS analysis as described in "materials and methods." Open traces show fluorescence of non-treated cells (1), Mal-βCD-treated cells (2), and Cho/Mal-βCD-treated cells after Mal-βCD treatment (3). The gray area shows the profile observed for isotype-matched control.

4. Discussion

Integrins, well-recognized as cell adhesion molecules, play a pivotal role in the bidirectional transmission of signals across the plasma membrane[1,32]. They serve as crucial structural and functional links between the cytoskeleton and ECM, facilitating intracellular signal transduction[33,34]. The adhesion of cells to the ECM via integrins is subject to regulation by the presence of divalent metal ions, including Ca^{2+}, Mg^{2+}, and Mn^{2+}.[3,5] Mn^{2+}, in particular, stands out as a potent effector in this context, effectively competing with Ca^{2+} and/or Mg^{2+} for binding to MIDAS found in the αI domain of the integrin α subunit and the βI domain in αI domain-less integrins[3,5,7-10]. The binding of Mn^{2+} induces a conformational shift in integrins, leading to the adoption of a ligand-affinity conformation and the subsequent expression of various cell phenotypes[5,11-13]. In our current investigation, we have corroborated that adding Mn^{2+} significantly enhances P-815 adhesion to the RGD matrix in Fisher's medium, containing 0.6 mM Ca^{2+} and 0.5 mM Mg^{2+}. Notably, the Mn^{2+}-induced P-815 adhesion surpassed that induced by PGE_2, a previously reported phenomenon, with Mn^{2+} achieving an approximately 40% increase compared to the approximately 20% increase achieved by PGE_2.[4] This reaffirms the potent adhesion-inducing capacity of Mn^{2+}.

Additionally, this study has unveiled that Co^{2+} and Ni^{2+} can mimic the weaker adhesion effect of Mn^{2+} on P-815. Both Ni^{2+} and Co^{2+} have been associated with the activation of adhesion molecules, including E-selectin and intracellular adhesion molecule-1, along with cytokines such as IL-6 and IL-8. This activation occurs through a mechanism involving the translation of the transcription factor NF-κB into the cell nucleus[35]. While we will delve into further details later, it is worth noting that the mode of action of Mn^{2+} on P-815 adhesion to the RGD matrix appears distinct from the nuclear mechanism attributed to Ni^{2+} and Co^{2+}, a notion that aligns with the work of Wagner et al.

Given that Mn^{2+} can readily oxidize to Mn^{3+} - Mn^{7+}, we examined the impact of various antioxidants on Mn^{2+}-induced P-815 adhesion to the RGD matrix. Interestingly, the inclusion of antioxidants such as ascorbic acid, cysteine, tocopherol, butylated hydroxytoluene, epigallocatechin gallate, and propyl gallate did not yield any discernible effects on Mn^{2+}-induced P-815 adhesion (data not shown).

This study is the first to elucidate the integrin molecules that mediate Mn^{2+}-induced adhesion in mast cell lines when interacting with the RGD matrix. We have determined that Mn^{2+}-induced P-815 adhesion is mediated by integrins α4β1 and αIIbβ3, with no significant alterations observed in the expression levels of these integrins on the cell surface. Conversely, Mn^{2+}-induced PMC adhesion to the RGD matrix hinges on integrins α4β1, α4β7, α5β1, and αIIbβ3. However, the study has yet to quantify changes in the expression of these integrins on the cell surface. These findings offer several noteworthy insights. Firstly, both P-815 and PMC adhere to the RGD matrix in a Mn^{2+}-dependent manner through integrins belonging to the same αI-less integrin subfamily. This subfamily encompasses α4, α5, αIIb, and αv subunits, with ligand recognition primarily occurring within the βI domain[10]. The βI domain is also the site where conformational changes are triggered by

divalent metal ions[7,8,10,12,36]. Furthermore, it is worth highlighting that both P-815 and PMC demonstrate Mn^{2+}-stimulated adhesion to the RGD matrix via common integrins α4β1 and αIIbβ3. This observation aligns with the study by Oki et al., which established that integrin αIIbβ3 in human and mouse mast cells, including mouse BMMC, facilitates adhesion and activation through interactions with fibrinogen[37]. Nonetheless, our research reveals a novel facet by demonstrating that Mn^{2+}-stimulated PMC adheres to the RGD matrix through distinct integrins, including α4β7 and α5β1, in addition to α4β1 and αIIbβ3. Exploring this divergence is challenging, as P-815 and PMC are distinct types of mast cells stemming from different progenitor cells[38], potentially influenced by the presence or absence of cancerous transformation. In light of the latter, it is worth noting that the relatively limited spectrum of integrins employed by P-815 for adhesion carries significance, considering that alterations in ECM adhesion capabilities during cancerous transformation are often associated with an increased propensity for metastasis.

Integrins play a crucial role in lipid rafts, and this interaction holds significance for initiating intricate signaling cascades upon cell adhesion to ECM[6]. Lipid rafts are known to house several integrins, with the active forms of integrins likely localizing within cholesterol-rich lipid rafts[39,40]. Consequently, the depletion of cholesterol by introducing Mal-βCD could potentially disrupt the structural integrity of lipid rafts and impede the signaling pathways they facilitate. In the current study, we found that Mn^{2+}-induced P-815 adhesion may be required for ECM/actin cytoskeleton connection, GPI-AP as a signal regulator, cAMP-dependent PKA activity, and cellular cholesterol. These results indirectly indicate the following experimental facts: Mn^{2+} has a role in the reaction of integrin engagement to stabilize actin projections[41,42], Mn^{2+} activates PKA-induced phosphorylation of cAMP response element-binding protein in PC12 cells[43], Mn^{2+} can stabilize PKA as an active conformation and assist in phosphoryl transfer using the catalytic subunit of cAMP/PKA[44], and Type I PKA in lipid rafts[28] phosphorylates the integrin α4 subunit of integrin α4β1[45,46]. Based on the results of these published studies, the following hypothesis regarding Mn^{2+} activity can be considered: Mn^{2+} administration may activate cAMP-dependent phosphorylation of PKA, inducing conformational changes via the phosphorylation of integrin subunits. As shown in the current data (Fig. 5) and previous papers[4,17], the PGE_2/cAMP system promotes P-815 adhesion, which was inhibited by H-89 administration but not by Y27632 and blebbistatin (data not shown). These results were similar to the effects of Mn^{2+} stimulation on P-815 adhesion, indicating that Mn^{2+}-induced P-815 adhesion activity is partially mediated by cAMP/PKA signals in addition to the direct conformational changes of ligand binding sites on the MIDAS of integrin subunits. This hypothesis is supported by the current experiment shown in Fig. 5, which shows that simultaneous administration of Mn^{2+} and PGE_2 has a more than additive effect on P-815 adhesion. In any case, we further need to clarify the series of routes by which Mn^{2+} induces conformational changes in integrins and activates the signaling pathways

in lipid rafts to promote cell adhesion to the RGD matrix.

It has been reported that CD47 interacts with integrins α4β1 and αvβ3, and resulting CD47/integrin complexes affect a range of cell functions, including adhesion, spreading, and migration[30,31]. However, CD47 had a weak correlation with neither Mn^{2+}-dependent P-815 adhesion in the present study nor PGE_2-dependent P-815 adhesion to the RGD matrix in a previous report[4]. These results suggested that the interaction of CD47/integrin with cell adhesion to the matrix varied depending on the cell type used in the experiment. However, we did not determine the effect of CD44 on Mn^{2+}-induced P-815 adhesion because CD44 is a major cell adhesion molecule expressed in cancer cells[47] and human BMMC[19]. On the other hand, Rho-ROCK-myosin signaling is an important regulator of cell adhesion to the ECM[48,49]. However, the adhesion of Mn^{2+}-induced P-815 to the RGD matrix was Rho-ROCK-myosin-independent from the experiment using Rho-ROCK-myosin inhibitors Y27632 and blebbistatin. Although lipid rafts are known to be involved in human neural cell adhesion[50] and human melanoma cell adhesion[51], whether Mn^{2+} is involved in these cell adhesion reactions remains to be determined.

5. Conclusion

Mn^{2+} promoted P-815 adhesion to the RGD matrix via activation of integrins α4β1 and αIIbβ3, and the responses are mediated by the activation of signaling pathways such as ECM/actin cytoskeleton connection, GPI-AP, cAMP-dependent PKA activity, and cellular cholesterol, which may be a reaction inside and outside of the lipid rafts. Contrarily, Mn^{2+}-induced adhesion of PMC occurs via integrins α4β7 and α5β1, in addition to integrins α4β1 and αIIbβ3. Furthermore, this study is the first to elucidate the signaling mechanism of Mn^{2+}-induced P-815 adhesion. The results of this study not only shed light on the molecular mechanisms of Mn^{2+}-induced cell adhesion but also have potential implications for mast cell-induced degradation of ECM and tissue remodeling and inflammation.

Conflicts of Interest Statement:

The authors have no conflicts of interest to declare.

Acknowledgements Statement:

We would like to thank Editage (www.editage.jp) for English language editing.

Author's Contributions:

Y.O. conceived and designed the study, performed the cellular experiments, analyzed the data, wrote and prepared the manuscript, and edited the manuscript; A.I. designed the study, analyzed the data, and edited the manuscript; K.U. and J.N. performed the cellular experiments, analyzed the data, and edited the manuscript.

Funding Statement:

None

References:

1. Hynes RO. Integrins: bidirectional, allosteric signaling machines. *Cell*. 2002; 110(6):673-687. doi:10.1016/S0092-8674(02)00971-6.

2. Humphries JD, Byron A, Humphries MJ. Integrin ligands at a glance. *J Cell Sci*. 2006; 119(19):3901-3903. doi:10.1242/jcs.03098.

3. Zhang K, Chen JF. The regulation of integrin function by divalent cations. *Cell Adh Migr*. 2012; 6(1):20-29. doi:10.4161/cam18702.

4. Okada Y, Nishikawa J, Semma M, Ichikawa A. Induction of integrin β3 in PGE_2-stimulated adhesion of mastocytoma P-815 cells to the Arg-Gly-Asp-enriched fragment of fibronectin. *Biochem Pharmacol*. 2011;81(7): 866-872. doi:10.1016/j.bcp.2011.01.010.

5. Anderson JM, Li J, Springer TA. Regulation of integrin α5β1 conformational states and intrinsic affinities by metal ions and the ADMIDAS. *Mol Biol Cell*. 2022;33(6): ar56:(Ar56). doi:10.1091/mbc.E21-11-0536.

6. Lietha D, Izard T. Roles of membrane domains in integrin-mediated cell adhesion. *Int J Mol Sci*. 2020; 21(15):5531-5549. doi:10.3390/ijms21155531.

7. Xiong JP, Stehle T, Diefenbach B, et al. Crystal structure of the extracellular segment of integrin αvβ3. *Science*. 2001;294(5541) :339-345. doi:10.1126/science.1064535.

8. Xiao T, Takagi J, Coller BS, Wang JH, Springer TA. Structural basis for allostery in integrins and binding to fibrinogen-mimetic therapeutics. *Nature*. 2004; 432(7013):59-67. doi:10.1038/nature02976.

9. Chen J-F, Salas A, Springer TA. Bistable regulation of integrin adhesiveness by a bipolar metal ion cluster. *Nat Struct Biol*. 2003; 10(12):995-1001. doi:10.1038/nsb1011.

10. Valdramidou D, Humphries MJ, Mould AP. Distinct roles of β1 metal ion-dependent adhesion site (MIDAS), adjacent to MIDAS (ADMIDAS), and ligand-associated metal-binding site (LIMBS) cation-binding sites in ligand recognition by integrin α2β1. *J Biol Chem*. 2008;283 (47):32704-32714. doi:10.1074/jbc.M802066200.

11. Gailit J, Ruoslahti E. Regulation of the fibronectin receptor affinity by divalent cations. *J Biol Chem*. 1988; 263(26):12927-12932. doi:10.1016/S0021-9258(18)37650-6.

12. Xiong JP, Stehle T, Zhang R, et al. Crystal structure of the extracellular segment of integrin αvβ3 in complex with an Arg–Gly–Asp ligand. *Science*. 2002; 296(5565):151-155. doi:10.1126/science.1069040.

13. Zhu J, Zhu J, Springer TA. Complete integrin headpiece opening in eight steps. *J Cell Biol*. 2013; 201(7):1053-1068. doi:10.1083/jcb.201212037.

14. Brown DA, London E. Structure and function of sphingolipid- and cholesterol-rich membrane rafts. *J Biol Chem*. 2000; 275(23):17221-17224. doi:10.1074/jbc.R000005200.

15. Krystel-Whittemore M, Dileepan KN, Wood JG. Mast cell: a multi-functional master cell. *Front Immunol* 2016; 6:620. doi:10.3389/fimmu.2015.00620.

16. Leist M, Sünder CA, Drube S, et al. Membrane-bound stem cell factor is the major but not only driver of fibroblast-induced murine skin mast cell differentiation. *Exp Dermatol*. 2017; 26(3):255-262. doi:10.1111/exd.13206. Epub February 9 2017.

17. Hatae N, Kita A, Tanaka S, Sugimoto Y, Ichikawa A. Induction of adherent activity in mastocytoma P-815 cells by the cooperation of two prostaglandin E_2 receptor subtypes,

EP3 and EP4. *J Biol Chem*. 2003; 278(20):17977-17981. doi:10.1074/jbc.M301312200.

18. Misiak-Tłoczek A, Brzezińska-Błaszczyk E. The regulation of mast cell migration. Part 1: cell adhesion molecules. *Postepy Hig Med Dosw (Online)*. 2007;61:485-492.

19. Pastwińska J, Walczak-Drzewiecka A, Kozłowska E, Harunari E, Ratajewski M, Dastych J. Hypoxia modulates human mast cell adhesion to hyaluronic acid. *Immunol Res*.2022;70(2):152-160. doi:10.1007/s12026-021-09228-x.

20. Tegoshi T, Nishida M, Arizono N. Expression and role of E-cadherin and CD103β7 (αEβ7 integrin) on cultured mucosal-type mast cells. *APMIS*. 2005; 113(2):91-98. doi:10.1111/j.1600-0463.2005.apm1130202.x.

21. Kuppe A, Evans LM, McMillen DA, Griffith OH. Phosphatidylinositol-specific phospholipase C of *Bacillus cereus*: cloning, sequencing, and relationship to other phospholipases. *J Bacteriol*. 1989; 171 (11):6077-6083. doi:10.1128/jb.171.11.6077-6083.1989.

22. Okada Y, Kubota Y, Koizumi K, Hizukuri S, Ohfuji T, Ogata K. Some properties and the inclusion behavior of branched cyclodextrins. *Chem Pharm Bull (Tokyo)*. 1988; 36(6):2176-2185. doi:10.1248/cpb.36.2176.

23. Sakanaka M, Tanaka S, Sugimoto Y, Ichikawa A. Essential role of EP3 subtype in prostaglandin E_2-induced adhesion of mouse cultured and peritoneal mast cells to the Arg–Gly–Asp-enriched matrix. *Am J Physiol Cell Physiol*. 2008; 295 (5):C1427-C1433. doi:10.1152/ajpcell.00218.2008.

24. Okada Y, Ueyama K, Nishikawa J, Semma M, Ichikawa A. Effect of 6-*O*-α-maltosyl-β cyclodextrin and its cholesterol inclusion complex on cellular cholesterol levels and ABCA1 and ABCG1 expression in mouse mastocytoma P-815 cells. *Carbohydr Res*. 2012;357:68-74. doi:10.1016/j.carres.2012.04.019.

25. Okada Y, Nishikawa J, Semma M, Ichikawa A. Role of lipid raft components and actin cytoskeleton in fibronectin-binding, surface expression, and *de novo* synthesis of integrin subunits in PGE_2- or 8-Br-cAMP-stimulated mastocytoma P-815 cells. *Biochem Pharmacol*. 2014; 88(3) 364-371. doi:10.1016/j.bcp.2014.01.039.

26. Pettit LD, Powell KJ. *IUPAC Stability Constant Database, IUPAC/Academic Software*. Otley, United Kingdom; 2003.

27. Schliwa M. Action of cytochalasin D on cytoskeletal networks. *J Cell Biol*. 1982; 92:79-91(1). doi:10.1083/jcb.92.1.79.

28. Raslan Z, Magwenzi S, Aburima A, Taskén K, Naseem KM. Targeting of type I protein kinase A to lipid rafts is required for platelet inhibition by the 3′,5′-cyclic adenosine monophosphate-signaling pathway. *J Thromb Haemost*. 2015; 13(9) 1721-1734. doi:10.1111/jth.13042.

29. Cheung AY, Li C, Zou YJ, Wu HM. Glycosylphosphatidylinositol anchoring: control through modification. *Plant Physiol*. 2014; 166(2):748-750. doi:10.1104/pp.114.246926.

30. Sick E, Jeanne A, Schneider C, Dedieu S, Takeda K, Martiny L. CD47 update: a multifaceted actor in the tumour microenvironment of potential therapeutic interest. *Br J Pharmacol*. 2012; 167(7):1415-1430. doi:10.1111/j.1476-5381.2012.02099.x.

31. Kaur S, Isenberg JS, Roberts DD. CD47 (cluster of differentiation 47). *Atlas Genet Cytogenet Oncol Haematol*. 2021; 25(2):83-102.

32. Luo BH, Carman CV, Springer TA. Structural basis of integrin regulation and signaling. *Annu Rev Immunol*. 2007; 25:619-647.doi:10.1146/annurev.immunol.25.022106.141618.

33. Clark EA, Brugge JS. Integrins and signal transduction pathways: the road taken. *Science*. 1995; 268 (5208):233-239. doi:10.1126/science.7716514.

34. Bershadsky A, Kozlov M, Geiger B. Adhesion-mediated mechanosensitivity: a time to experiment, and a time to theorize. *Curr Opin Cell Biol*. 2006; 18(5):472-481. doi:10.1016/j.ceb.2006.08.012.

35. Wagner M, Klein CL, van Kooten TG, Kirkpatrick CJ. Mechanisms of cell activation by heavy metal ions. *J Biomed Mater Res*. 1998; 42(3):443-452. doi:10.1002/(sici)1097-4636(19981205)42:3<443::aid-jbm14>3.0.co;2-h.

36. Mould AP, Humphries MJ. Regulation of integrin function through conformational complexity: not simply a knee-jerk reaction? *Curr Opin Cell Biol*. 2004; 16(5):544-551. doi:10.1016/j.ceb.2004.07.003.

37. Oki T, Kitaura J, Eto K, et al. Integrin αIIbβ3 induces the adhesion and activation of mast cells through interaction with fibrinogen. *J Immunol*. 2006; 176(1):52-60. doi:10.4049/jimmunol.176.1.52.

38. Malbec O, Roget K, Schiffer C, et al. Peritoneal cell-derived mast cells: an in vitro model of mature serosal-type mouse mast cells. *J Immunol*. 2007; 178(10):6465-6475. doi:10.4049/jimmunol.178.10.6465.

39. Bodin S, Soulet C, Tronchère H, et al. Integrin-dependent interaction of lipid rafts with the actin cytoskeleton in activated human platelets. *J Cell Sci*. 2005; 118(4):759-769. doi:10.1242/jcs.01648.

40. Bi J, Wang R, Zeng X. Lipid rafts regulate the lamellipodia formation of melanoma A375 cells via actin cytoskeleton-mediated recruitment of β1 and β3 integrin. *Oncol Lett*. 2018;16(5):6540-6546. doi:10.3892/ol.2018.9466.

41. Zaidel-Bar R, Cohen M, Addadi L, Geiger B. Hierarchical assembly of cell-matrix adhesion complexes. *Biochem Soc Trans*. 2004;32():416-420. doi:10.1042/BST0320416.

42. Zimerman B, Volberg T, Geiger B. Early molecular events in the assembly of the focal adhesion-stress fiber complex during fibroblast spreading. *Cell Motil Cytoskeleton*. 2004; 58(3):143-159. doi:10.1002/cm.20005.

43. Zhu G, Liu Y, Zhi Y, et al. PKA- and Ca^{2+}-dependent p38 MAPK/CREB activation protects against manganese-mediated neuronal apoptosis. *Toxicol Lett*. 2019;309:10-19. doi:10.1016/j.toxlet.2019.04.004.

44. Knape MJ, Ballez M, Burghardt NC, et al. Divalent metal ions control activity and inhibition of protein kinases. *Metallomics*. 2017;9(11):1576-1584. doi:10.1039/c7mt00204a.

45. Howe AK. Regulation of actin-based cell migration by cAMP/PKA. *Biochim Biophys Acta*. 2004; 1692 (2-3):159-174. doi:10.1016/j.bbamcr.2004.03.005.

46. Lim CJ, Kain KH, Tkachenko E, et al. Integrin-mediated protein kinase A activation at the leading edge of migrating cells. *Mol Biol Cell*. 2008; 19(11):4930-4941. doi:10.1091/mbc.e08-06-0564.

47. Thomas L, Byers HR, Vink J, Stamenkovic I. CD44H regulates tumor cell migration on hyaluronate-coated substrate. *J Cell Biol*.

1992;118(4):971-977. doi:10.1083/jcb.118.4.971.

48. Bhadriraju K, Yang M, Alom Ruiz SA, Pirone D, Tan J, Chen CS. Activation of ROCK by RhoA is regulated by cell adhesion, shape, and cytoskeletal tension. *Exp Cell Res*. 2007; 313(16):3616-3623. doi:10.1016/j.yexcr.2007.07.002.

49. Schiller HB, Hermann MR, Polleux J, et al. β1- and αv-class integrins cooperate to regulate myosin II during rigidity sensing of fibronectin-based microenvironments. *Nat Cell Biol*. 2013; 15(6):625-636. doi:10.1038/ncb2747.

50. Povlsen GK, Ditlevsen DK. The neural cell adhesion molecule NCAM and lipid rafts. *Adv Exp Med Biol*. 2010; 663:183-198. doi:10.1007/978-1-4419-1170-4_12.

51. Wang R, Bi J, Ampah KK, Ba X, Liu W, Zeng X. Lipid rafts control human melanoma cell migration by regulating focal adhesion disassembly. *Biochim Biophys Acta*. 2013; 1833(12):3195-3205. doi:10.1016/j.bbamcr.2013.09.007.